in favor of highly branched huge molecules. Thus a decrease in the mean value of $\bar{\zeta}$ means that ζ of individual molecules decreases when the degree of cross-linking increases. This is confirmed by light scattering on the high molecular weight fraction of an irradiated sample shown in Figure 5. For the fraction, Zimm plot curves upward, which means that $\bar{\zeta} < 1$ whereas the nonfractionated sample has $\bar{\zeta} > 1$.

References and Notes

(1) Flory, P. J. *J. Am. Chem. Soc.* **1941**, *63*, 3097.
(2) Stockmayer, W. H. *J. Chem. Phys.* **1944**, *12*, 125.
(3) de Gennes, P. G. *J. Phys. (Paris) Lett.* **1977**, *38*, L355.
(4) Daoud, M *J. Phys. (Paris) Lett.* **1979**, *40*, L201.
(5) For a comparison between Flory–Stockmayer and percolation theory see, for example, the review article by: Stauffer, D.; Coniglio, A.; Adam, M. *Adv. Polym. Sci.* **1982**, *44*, 103.
(6) Charlesby, A.; Alexander, P. *J. Chim. Phys.* **1955**, *52*, 694. Alexander, P.; Charlesby, A. *J. Polym. Sci.* **1957**, *23*, 355.
(7) Henglein, A.; Schneider, C. *Z. Phys. Chem. (Frankfurt/Main)* **1958**, *18*, 56.
(8) Wippler, C. *J. Polym. Sci.* **1958**, *29*, 585. Rougée, M.; Wippler, C. In Proceedings of the International Symposium on Macromolecular Chemistry, Wiesbaden, 1959. Rougée, M. Thèse d'Etat, Université Louis Pasteur, Strasbourg, 1963.
(9) For a review of early literature, see: Chapiro, A. "Radiation Chemistry of Polymeric Systems"; Interscience: New York, 1962; Chapter XI.
(10) Bastide, J. Thèse d'Etat, Université Louis Pasteur, Strasbourg, 1984.
(11) Adam, M.; Delsanti, M.; Okasha, R.; Hild, G. *J. Phys. (Paris), Lett.* **1979**, *40*, L539.
(12) Gautier-Manuel, B.; Guyon, E. *J. Phys. (Paris), Lett.* **1980**, *41*, L503.
(13) Ankrim, M. Thèse d'Etat, Université Louis Pasteur, Strasbourg, 1984.
(14) Daoud, M.; Family, F.; Jannink, G. *J. Phys. (Paris) Lett.* **1984**, *45*, 193.
(15) Shinbo, K.; Miyake, Y. *J. Phys. Soc. Jpn.* **1980**, *48*, 2084.
(16) Gordon, M.; Kajiwara, K.; Peniche-Covas, C. A. L.; Ross-Murphy, S. B. *Makromol. Chem.* **1975**, *176*, 2415.
(17) Schosseler, F.; Leibler, L. *J. Phys. (Paris), Lett.* **1984**, *45*, L501-507.
(18) Stockmayer, W. H. *J. Chem. Phys.* **1943**, *11*, 45.
(19) Pis'men, L. M.; Kuchanov, S. I. *Vysokomol. Soedin., Ser. A* **1971**, *13*, 791.
(20) Dusek, K. *Polym. Bull.* **1979**, *1*, 523.
(21) Ziff, R. M. *J. Stat. Phys.* **1980**, *23*, 241.
(22) Ziff, R. M.; Stell, G. *J. Chem. Phys.* **1980**, *73*, 3492.
(23) Von Schulthess, G. K.; Benedek, G. B.; de Blois, R. W. *Macromolecules* **1980**, *13*, 939.
(24) de Gennes, P.-G.; G. F. P. Meeting on Gels, Strasbourg, 1983 (unpublished).
(25) Charlesby, A. *Proc. R. Soc. (London), Ser. A* **1955**, *222*, 542.
(26) Parisi, G.; Sourlas, N. *Phys. Rev. Lett.* **1981**, *46*, 871.
(27) Daoud, M.; Joanny, J.-F. *J. Phys. (Paris)* **1981**, *42*, 1359.
(28) Stauffer, D. *Phys. Rep.* **1979**, *54*, 2.
(29) Leyvraz, F.; Tschudi, H. R. *J. Phys. A, Math. Gen.* **1982**, *15*, 1951. Ziff, R. M.; Hendriks, E. M.; Ernst, M. H. *Phys. Rev. Lett.* **1982**, *43*, 593.
(30) Burchard, W.; Kajiwara, K.; Gordon, M.; Kalal, J.; Kennedy, J. W. *Macromolecules* **1973**, *6*, 642. Whitney, R. S.; Burchard, W. *Makromol. Chem.* **1980**, *181*, 869. Schmidt, M.; Burchard, W. *Macromolecules* **1981**, *14*, 370. Bantle, S.; Hasslin, H. W.; ter Meer, H. V.; Schmidt, M.; Burchard, W. *Polymer* **1982**, *23*, 1889.
(31) Munch, J. P.; Ankrim, M.; Hild, G.; Okasha, R.; Candau, S. *Macromolecules* **1984**, *17*, 110. Candau, S.; Ankrim, M.; Munch, J. P.; Rempp, P.; Hild, G.; Okasha, R., preprint, 1984.
(32) Witten, T. A.; Schäfer, L. *J. Chem. Phys.* **1981**, *74*, 2582.

Conformational Characteristics of Poly(1-alkenes). Flexible Side Groups and the Limits of Simple Rotational Isomeric State Models

Heinz Wittwer and Ulrich W. Suter*

Institut für Polymere, ETH-Zürich, CH-8092 Zürich, Switzerland, and Department of Chemical Engineering, Massachusetts Institute of Technology, Cambridge, Massachusetts 02139.

Received June 14, 1984

ABSTRACT: Rotational isomeric state models were constructed, based on the model for poly(propylene) with five states per bond, and assuming mutually independent side groups, for poly(1-butene) (P1B), poly(1-pentene) (P1P), poly(4-methyl-1-pentene) (P4MP), and poly[(*S*)-4-methyl-1-hexene] (PS4MH). Values for the unperturbed dimensions were calculated and found to be in good agreement with experiment for P1B and P1P, and poor agreement with experiment for P4MP and PS4MH. The reason for the poor agreement for P4MP and PS4MH was found to lie in the mutual interdependence between side groups. A remedy is offered by direct numerical integration; this approach, however, is limited by the amount of computational effort necessary that increases exponentially with the number of rotational degrees of freedom in the side chains. Conformational statistics for PS4MH, the optically active polymer investigated, were analyzed.

Introduction

The conformation of poly(1-alkenes) with articulated side chains has been the subject of many investigations. Crystal structure analysis of partially crystalline, isotactic samples revealed the helical nature of these chains shortly after the first stereoregular synthesis.[1,2] Since then very detailed crystal structures have been obtained, and polymorphisms have been observed in several cases (see ref 3–9 and references cited therein). Calculations of the intramolecular potential energy of regular conformations of poly(propylene) (PP) as a function of the torsion angles were first performed by Natta, Corradini, and Ganis.[10] Their results were confirmed,[11] and the method was refined and extended to isotactic polymers with longer side chains.[3,12-14] Agreement between experiment and calculations was very good. These experiments and the corresponding computations indicate a strong influence of the side chains on the minimum-energy conformation with regular repetition of torsion angles. Unfortunately, these calculations are not directly applicable to polymers in melt or in solution.

Experimental results on the conformational characteristics of isotactic and atactic poly(1-alkenes) in solution are also numerous. Foremost among them are values for the characteristic ratio of the unperturbed end-to-end distance and its temperature coefficient;[15-26] they comprise

0024-9297/85/2218-0403$01.50/0

Table I
Parameters Used in Energy Calculations

		bond length, Å
C–C		1.53
C–H		1.10
		bond angle, deg
at CH_2	C–C–C	114.0
	C–C–H	108.5
	H–C–H	108.5
at CH	C–C–C	112.0
	C–C–H	106.8

Lennard-Jones 6–12 Potential Energy Constants

pair	$10^{-3}a$, kcal mol^{-1} Å^{12}	c, kcal mol^{-1} Å^{6}
C, C	398	366
C, H	57	128
C, CH_3	968	643
H, H	7.3	47
H, CH_3	148	229
CH_3, CH_3	2329	1137

results for poly(propylene) (PP), poly(1-butene) (P1B), poly(1-pentene) (P1P), poly(4-methyl-1-pentene) (P4MP), and poly[(*S*)-4-methyl-1-hexene] (PS4MH). The chiral side group of the last-mentioned polymer generates net optical activity, and optical rotation has been determined for atactic as well as isotactic chains.[27-29] Theoretical attempts to account for these results have also been many. It was recognized some time ago that the contributions of the side groups to the partition function of the chain strongly influences the statistics of the backbone conformations and that for chiral side groups the populations of enantiomeric pairs of main-chain conformations are not equal.[27-32] In these early investigations helical conformations were primarily considered. A comprehensive treatment in a full rotational isomeric state (RIS) model was introduced by Abe;[33-35] an equivalent model was used by Mattice.[36,37] Abe's results were obtained by using three states per bond and statistical weight parameters from previous work on poly(ethylene) and "simple" vinyl polymers.[38-40] Calculations agreed with experiment only when it was assumed that the so-called "highly isotactic" polymers contain at least 2% racemo diads for PP and at least 7% racemo diads for P1B and P1P, values we consider today unrealistically high. More recently, detailed consideration of PP revealed that a realistic RIS model for this polymer requires five states per bond and that the statistical weight parameters are larger than previously expected.[41]

In the present work we present application of the five-state model to P1B, P1P, P4MP, and PS4MH. To this end we investigate first the potential energy of diads as a function of the main-chain torsion angles, the side chain being adjusted to yield minimum energy. Then Abe's method[33] is used in the context of these results. Finally, the possible interdependence of the conformations of neighboring side groups is considered (such interdependences are assumed to be negligible in Abe's method, which considers interactions of first and second order only), and conclusions are drawn as to the limitations of simple RIS schemes.

Structural Model

Calculations were performed on diads and triads (see Figure 1), bond lengths and bond angles being fixed at the values given in Table I.[41,42] Methyl groups in side chains are represented as single spheres of van der Waals radius 2.0 Å;[42] otherwise atoms are considered individually.

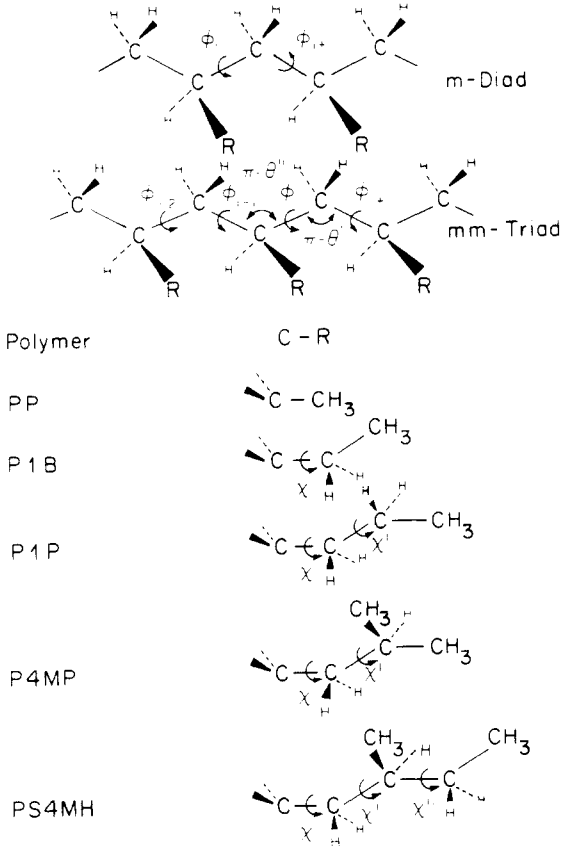

Figure 1. Diads and triads of the polymers considered (all torsion angles are set to zero).

The total conformational potential energy is assumed to be the sum of interactions between nonbonded atoms ("van der Waals interactions") and from "intrinsic torsional energy". Nonbonded interactions between atoms separated by more than two bonds are calculated with a Lennard-Jones 6–12 pair energy function which is truncated at an interatomic distance of 5 Å, replaced in the neighborhood of the cutoff (i.e., between 4.5 and 5.5 Å) by a cubic polynomial.[42,43] This truncation roughly approximates the effect of surrounding molecules on the pair interaction energy of nonbonded atoms in condensed phase. A threefold intrinsic torsional energy function with a barrier of 2.8 kcal mol^{-1} is assigned to each C–C bond.[38]

For backbone torsion angles the all-trans position indicated in Figure 1 corresponds to $\phi_j = 0$. The sign of the torsion angles is chosen to give positive values for g conformations and negative values for $\bar{g}$ conformations.[44] For the side chains the conformations for which χ, χ', and χ'' are zero are shown in Figure 1. Right-handed rotations in the side groups produce positive signs.

Potential Energy Maps

Maps of the potential energy of meso and racemo diads of P4MP were calculated by using the model described above. The conformational energy was computed for given values of the main-chain torsion angles ϕ_i and ϕ_{i+1}, the side-group torsion angles χ_{i-1}, χ'_{i-1}, χ_{i+1}, and χ'_{i+1} being adjusted with a quasi-Newton method to give the minimum possible energy. Contour maps of this energy as a function of ϕ_i and ϕ_{i+1} were produced, based on grids with intervals of 10°. To assure that the absolute minimum with respect to all χ's was found, the minimization process has been carried out with several different sets of starting values. The resulting contour maps are shown in Figures 2 and 3. Lines of equal energy are drawn at an interval of 1 kcal mol^{-1} relative to the absolute minimum (|tt|

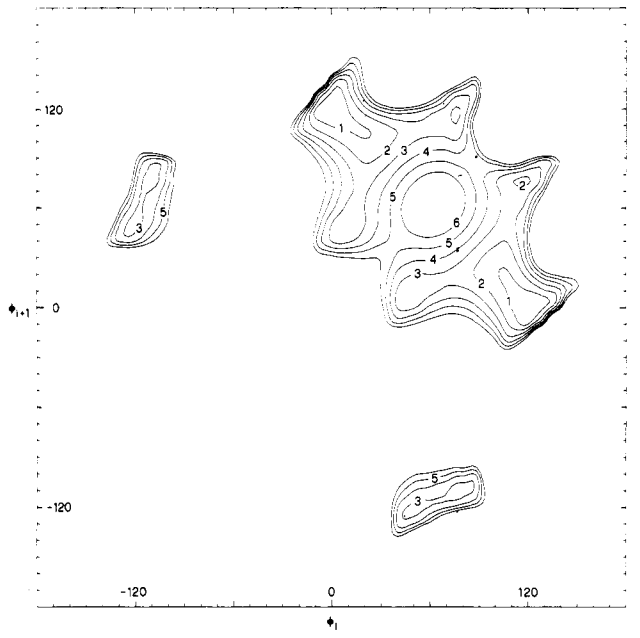

Figure 2. Conformational potential energy contour map for a meso diad of P4MP. For each main-chain bond angle pair (ϕ_i,ϕ_{i+1}) the side-chain torsion angles were adjusted to give absolute minimum energy. Contours are drawn at intervals of 1 kcal mol^{-1} relative to the racemo-|tt| minimum (see Figure 3).

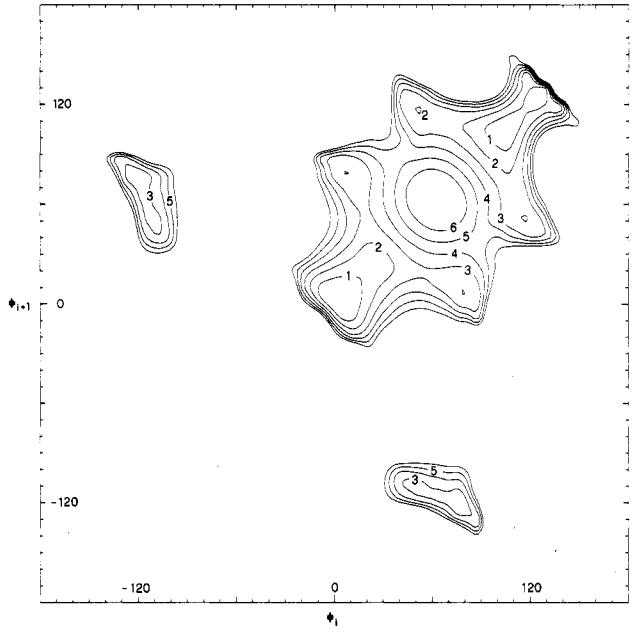

Figure 3. Conformational potential energy contour map for a racemo diad of P4MP. See legend to Figure 2.

conformation of the racemo diad). Blank areas have energies higher than 6 kcal mol^{-1}.

Both maps thus obtained for P4MP diads show 10 local low-energy minima; they are essentially identical with the maps for PP,[41] the differences being insignificant. We conclude therefore that the influence of the side chains in their optimum conformation on the main-chain potential energy of diads is negligible. From this and inspection of models we deduce that the shape of the conformational energy maps of poly(1-alkenes) will be identical with those for PP as long as the side chain contains a CH_2 in the α-position and its β-carbon is not quaternary. In any of the 10 troughs identifiable in Figures 2 and 3 (each), representing the accessible chain conformations of a diad of such a polymer, the side groups can always be accommodated in such a way as not to cause an increase in energy.

The case of PS4MH illustrates the validity of this conclusion. Here the strict symmetry about the line $\phi_i = \phi_{i+1}$ in the meso map is lost because of the chiral center in the side chain, but deviations from this symmetry should be minimal. Indeed, calculations of these deviations show them to be small; the difference between the energies in the minima conformations of |tg| and |gt|, for instance, i.e., between helical sections of opposite handedness, is ca. 0.2 kcal mol^{-1}.

The maps of the racemo and meso diads in Figures 2 and 3 can almost be superposed by a simple rotation of the coordinate system by 90° about $\phi_i = \phi_{i+1} \approx 60°$. This again indicates that the structure of the side chain has only a small influence on the shape of the maps, which is primarily determined by the structural segment

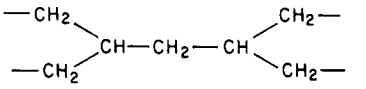

present in the meso as well as in the racemo diad.

In summary, 10 rotational isomers are found at the same backbone torsion angles in all the meso and racemo diads of the class of polymers considered here. The structure of the side chain can greatly influence their relative populations, however, as will be demonstrated below.

Statistical Weight Matrices Following Abe's Method

Statistical Weight Matrices. Following Abe[33] the contributions of the side chain to the conformational partition function of the chain are incorporated in the interdiad matrix $\mathbf{U}'$ only. The intradiad matrices $\mathbf{U}''_m$ and $\mathbf{U}''_r$ for all polymers considered here can be identified with those for PP[41] (Flory's notation is used[40])

$$\mathbf{U}''_m = \begin{bmatrix} 0 & \eta\omega^* & 0 & \eta & 0 \\ \eta\omega^* & 0 & 0 & 0 & \tau\omega^* \\ 0 & 0 & 0 & \omega^* & \tau\omega^* \\ \eta & 0 & \omega^* & 0 & 0 \\ 0 & \tau\omega^* & \tau\omega^* & 0 & 0 \end{bmatrix}$$

$$\mathbf{U}''_r = \begin{bmatrix} \eta^2 & 0 & \eta\omega^* & 0 & 0 \\ 0 & 0 & 0 & \omega^* & \tau\omega^* \\ \eta\omega^* & 0 & 0 & 0 & \tau\omega^* \\ 0 & \omega^* & 0 & 1 & 0 \\ 0 & \tau\omega^* & \tau\omega^* & 0 & 0 \end{bmatrix} \quad (1)$$

where η and τ are first-order statistical weights describing the weight of t and $\bar{g}$ with respect to g. ω^* is associated with a "four-bond interaction" and is an effective second-order parameter.

For PP the interdiad matrix $\mathbf{U}'$ is[41]

$$\mathbf{U}'_{PP} = \begin{bmatrix} 1 & 1 & 1 & 1 & 1 \\ 1 & 1 & 1 & 1 & 1 \\ 1 & 1 & 0 & 0 & 1 \\ 1 & 1 & 0 & 0 & 1 \\ 1 & 1 & 1 & 1 & 0 \end{bmatrix} \quad (2)$$

Abe multiplied every element in $\mathbf{U}'$, u_{kl}, with a statistical weight factor β_{kl}, attributable to the side chain

$$\beta_{kl} = \mathbf{S}_{[1}(kl)\mathbf{S}_2 \ldots \mathbf{S}_j \ldots \mathbf{S}_{n]} = \mathbf{S}_{[1}(kl)^{(n)} \quad (3)$$

where $\mathbf{S}_j$ is the statistical weight matrix for the jth bond in the side group which consists of n relevant bonds. The rotational isomeric state of the first side-group bond (angle χ) is named according to the relative position of the following bond, in reference to the preceding bond of the

Table II
$S_{[1}(kl)$ for all Combinations of Backbone Rotational Isomeric States of Bonds $i - 1$ and i

	bond i				
	l = t	l = t*	l = g*	l = g	l = $\bar{g}$
bond $i - 1$					
k = t	[τ 0 ω ω 0]	[τ 0 ω 0 ω]	[τ 0 ω 0 1]	[τ 0 ω 0 1]	[$\tau\omega$ 0 ω 0 1]
k = t*	[τ ω 0 ω 0]	[τ ω 0 0 ω]	[τ ω 0 0 1]	[τ ω 0 0 1]	[$\tau\omega$ ω 0 0 1]
k = g*	[τ 1 0 ω 0]	[τ 1 0 0 ω]	[τ 1 0 0 1]	[τ 1 0 0 1]	[$\tau\omega$ 1 0 0 1]
k = g	[τ 1 0 ω 0]	[τ 1 0 0 ω]	[τ 1 0 0 1]	[τ 1 0 0 1]	[$\tau\omega$ 1 0 0 1]
k = $\bar{g}$	[$\tau\omega$ 1 0 ω 0]	[$\tau\omega$ 1 0 0 ω]	[$\tau\omega$ 1 0 0 1]	[$\tau\omega$ 1 0 0 1]	[$\tau\omega^2$ 1 0 0 1]

main chain, e.g., bond $i + 1$ for the second side group in a diad (see Figure 1).

For P1B the side-chain torsion angle χ assumes essentially three values, 0°, +130°, and −130°, corresponding to states g^+, g^-, and t, respectively. Anticipating the necessity for five torsional states for the polymers with longer side chains, considered below, we introduce five different torsion angles

$$\chi = (0, +130°, +170°, -170°, -130°) \quad (4)$$

corresponding to states g^+, g^-, g^-_*, t_*, and t, in this order, according to Abe's convention.[33] Using the statistical weight parameter τ for the g^+ state ($\chi = 0$), and the weight ω for conformations where the methyl group is juxtaposed to CHR ("four-bond interaction"), the statistical weight matrices of order 1×5 of the side-group bond, for each of the 25 combinations of main-chain rotational isomeric states of bond $i - 1$ and i, are given in Table II. With

$$\mathbf{S}_{n]} = \text{col}\ (1,1,1,1,1) \quad (5)$$

and $\beta_{kl} = \mathbf{S}_{[1}(kl)\mathbf{S}_{n]}$ we obtain $\mathbf{U}'$ for P1B multiplying every element in $\mathbf{U}'_{PP}$ (eq 2) with the appropriate β_{kl}, viz. $[u'_{P1B}]_{kl} = [u'_{PP}]_{kl}\beta_{kl}$. Thus

$$\mathbf{U}' = \begin{bmatrix} a & a & b & b & c \\ a & a & b & b & c \\ b' & b' & 0 & 0 & d \\ b' & b' & 0 & 0 & d \\ c' & c' & d & d & 0 \end{bmatrix} \quad (6)$$

with

$$a = \tau + 2$$
$$b = b' = 1 + \tau + \omega$$
$$c = c' = 1 + \omega + \tau\omega$$
$$d = 2 + \tau\omega \quad (7)$$

In P1P the first side-group bond assumes the same rotational isomeric states as the analogous bond in P1B, and the statistical weight matrices from Table II apply accordingly. The five states of the second bond are assigned at 0° (t), +70° (g^+_*), +120° (g^+), −120° (g^-), and −70° (g^-_*). Taking σ as first-order statistical weight for the gauche states with respect to trans,[45] the statistical weight matrix for the second side bond is

$$\mathbf{S}_2 = \begin{bmatrix} 1 & \sigma\omega & 0 & 0 & \sigma\omega \\ 1 & \sigma\omega & 0 & \sigma & 0 \\ 1 & 0 & \sigma\omega & \sigma & 0 \\ 1 & 0 & \sigma & \sigma\omega & 0 \\ 1 & 0 & \sigma & 0 & \sigma\omega \end{bmatrix} \quad (8)$$

Here $\beta_{kl} = \mathbf{S}_{[1}(kl)\mathbf{S}_2\mathbf{S}_{n]}$, where $\mathbf{S}_{n]}$ comes from eq 5 and $[u'_{P1P}]_{kl} = [u'_{PP}]_{kl}\beta_{kl}$. $\mathbf{U}'_{P1P}$ is then given by eq 6 with

$$a = \tau + 2\omega + 2\sigma\omega + 2\sigma\tau\omega$$
$$b = b' = 1 + \sigma + \tau + \omega + 2\sigma\omega + 2\sigma\tau\omega$$
$$c = c' = 1 + \sigma + \omega + 2\sigma\omega + \tau\omega$$
$$d = 2 + 2\sigma + 2\sigma\omega + \tau\omega \quad (9)$$

neglecting terms in ω^2.

For P4MP the rotational isomeric states of the second side-chain torsion angle (χ') are located at values of 10° (t), 50° (t*), 70° (g*), 110° (g), and −120° ($\bar{g}$), as for a main chain of PP. Torsion angles for the first bond in the side chain are the same as those in eq 4; the corresponding statistical weight matrices are those from Table II. When the statistical weight matrix $\mathbf{S}_2$ and the factors β_{kl} are evaluated as above (terms in ω^2 again being neglected), $\mathbf{U}'_{P4MP}$ is given by eq 6 with

$$a = 2\omega + 2\tau\omega$$
$$b = b' = 1 + 2\omega + 3\tau\omega$$
$$c = c' = 1 + 2\omega + \tau\omega$$
$$d = 2 + 2\omega + 2\tau\omega \quad (10)$$

No distinction was made between ω, as it is used for *n*-alkanes,[38] and ω^* (as used in the conformational analysis of PP) since their numerical values are very similar.

For PS4MH the first two side-chain torsion angles, χ and χ', are assigned rotational isomeric states as for P4MP above, and the same statistical weight matrices apply. For the third bond only three rotational isomeric states need be considered, i.e., t (−10°), g (−110°), and $\bar{g}$ (+120°), where the torsion angles are measured in a right-handed system, but the states are labeled as in PP. $\mathbf{S}_3$ is then a 5×3 matrix, and $\mathbf{S}_{n]} = \text{col}\ (1,1,1)$. $\mathbf{U}'_{PS4MH}$ is obtained from eq 6 with

$$a = \omega + 2\eta\omega + 4\tau\omega + \eta\tau\omega + 2\tau^2\omega$$
$$b = 1 + 3\omega + 2\eta\omega + \tau + 6\tau\omega + \eta\tau\omega + 2\tau^2\omega$$
$$b' = 2\eta + 2\omega + \eta\tau + 7\tau\omega + 2\tau^2\omega$$
$$c = 1 + 3\omega + 2\eta\omega + \tau + 3\tau\omega + \eta\tau\omega$$
$$c' = 2\eta + 2\omega + \eta\tau + 4\tau\omega$$
$$d = 1 + 2\eta + 4\omega + \tau + \eta\tau + 6\tau\omega \quad (11)$$

terms in ω^2 and higher powers of ω being neglected.

Characteristic Ratios. For the calculation of the characteristic ratio, $C_\infty = \lim_{n\to\infty} \langle r^2\rangle_0/nl^2$, standard generator matrix methods were used.[46] Bond angles were set according to Table I and torsion angles as for PP,[41] i.e., 15° (t), 50° (t*), 70° (g*), 105° (g), and −115° ($\bar{g}$). The statistical weights σ, η, τ, and $\omega = \omega^*$ were taken as[38,41]

$$\sigma = 1.0\ \exp(-250/T)$$
$$\eta = 1.0\ \exp(-35/T)$$
$$\tau = 0.5\ \exp(-250/T)$$
$$\omega = \omega^* = 0.9\ \exp(-900/T) \quad (12)$$

with T in kelvins. At 400 K, for instance, $\sigma = 0.53$, $\eta = 0.92$, $\tau = 0.27$, and $\omega = \omega^* = 0.09$.

Calculated characteristic ratios for *atactic* PP with Bernoullian distribution of the diad configuration and $(m) \approx 0.5$ were in good agreement with available experimental

Table III
Temperature Coefficients of the Characteristic Ratio, $\lim_{n\to\infty} \langle r^2\rangle_0/nl^2$, for Atactic PP, P1B, P1P, P4MP, and PS4MH

polymer	10^3(d ln $\langle r^2\rangle_0$/dT), K^{-1} calcd	exptl (ref)	method
PP	−0.9	−1.8 (22)	d ln $[\eta]_\theta$/dT (306–419 K)
		−0.1 (17)	
P1B	−0.1	−0.4 (22)	d ln $[\eta]_\theta$/dT (295–414 K)
		+0.5 (18)	$(df/dT)_P$ (413–473 K)
P1P	−0.1	−0.3 (22)	d ln $[\eta]_\theta$/dT (306–421 K)
		+0.5 (18)	$(df/dT)_P$ (313–413 K)
P4MP	−0.01		
PS4MH	−0.2		

values.[41] Calculations with the same configurational statistics for the other chains considered in this paper yield, independent of the structure of the side group, values of C_∞ of ca. 4.5 for $(m) = 0.5$; experimental values are available for atactic P1B and P1P, and they are ca. 7 and 8, respectively.[22] Since little is known about the distribution of diad configuration of these stereoirregular samples, the differences between experiments and computations are probably insignificant (exploratory calculations show that C_∞ is sensitive to the distribution of diad configuration). Regardless of these distributions the calculated temperature coefficients d ln $\langle r^2\rangle_0$/dT for the atactic polymers are always negative. Values are listed in Table III. These values roughly match the experimental data obtained by viscosity measurements at different temperatures.

Calculated values for the *isotactic* polymers are shown as lines in Figure 4. Experimental results are indicated by dots; citations can be found in the legend. For isotactic PP and isotactic P1B agreement of the calculations with experiment is good. For isotactic P1P the magnitude of the calculated characteristic ratio is in satisfactory agreement with experiment; the magnitude of the calculated temperature coefficient of C_∞ is larger, however, than that found experimentally by Moraglio and Gianotti.[22,47] The characteristic ratio of isotactic P4MP has been determined by two groups: Tani, Hamada, and Nakajima[28] estimated values for C_∞ that are about twice as large as those of Neuenschwander and Pino,[24] who held the insufficient range of molecular masses of the samples used by Tani et al. responsible for the discrepancy. Our calculations agree satisfactorily with Neuenschwander and Pino's datum.

For PS4MH, however, these calculations do not agree with experiment. One might suspect that the statistical weights assigned to the third side-chain bond (χ''), the only structural difference compared to P4MP, are responsible for the failure of the calculations to reproduce the experimental values. The parameter η, weighting t vs. g for the third bond, might not be appropriate. However, calculations with η set to unity in $\mathbf{U}'_{PS4MH}$ (eq 11) yield the results represented by the dashed line in Figure 4; the change in C_∞ with changing η is marginal, indicating that the discrepancy between experiments and calculations do not originate in subtleties of the treatment of the last bond, but must have other reasons.

The failure of the simple five-state scheme to account for the conformational statistics of PS4MH led us to expect that side groups of this size cannot be treated independently of one another (in the method used here it is assumed that the contribution of a side group to the conformational partition function of the chain is independent of neighboring side groups). Obviously, neighboring long flexible side chains will mutually exclude some of their accessible

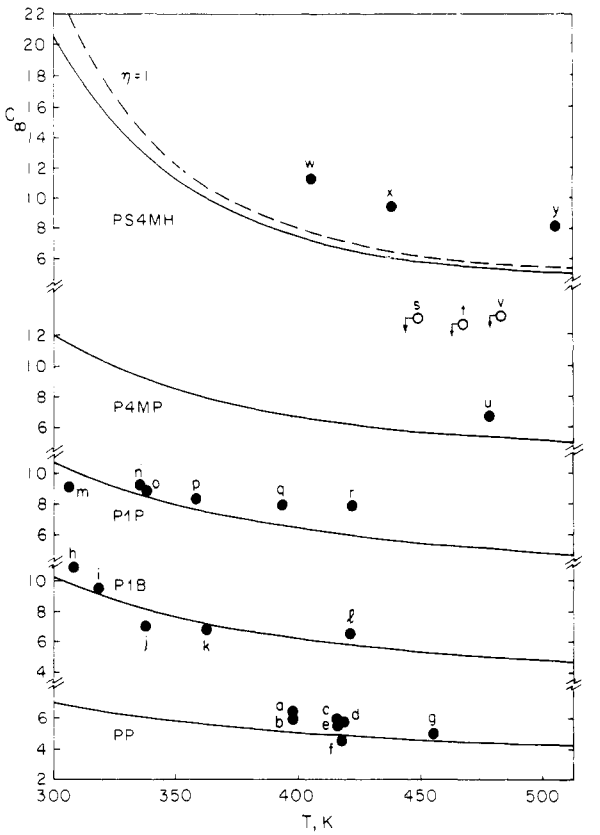

Figure 4. Characteristic ratios, $\lim_{n\to\infty} \langle r^2\rangle_0/nl^2$, for isotactic PP, P1B, P1P, P4MP, and PS4MH, calculated with the simple five-state scheme (Abe's method); see text for details. Points represent experimental data and are taken from (a, c, g) ref 19, (b, e, j–m, o–r) ref 22 and references cited therein, (d) ref 15, (f) ref 20, (h) ref 21, (i) ref 16, (n) ref 18, (s, t, v) ref 23, (u, w–y) ref 24.

space; in the above calculations which consider only first- and second-order interactions, however, they were effectively allowed to overlap. PS4MP might be a polymer where such overlaps occur to different extent in conformations of otherwise low energy and therefore need be accounted for.

Statistical Weight Matrices by Direct Integration; Method and Application to P4MP and PS4MH

Method. The above-mentioned failure of the simple five-state scheme to yield correct values for the characteristic ratio, C_∞, of isotactic PS4MH led us to proceed to a method for the evaluation of conformational averages that takes proper account of interdependences between side-group conformations. This method rests on the computation of statistical weight matrices by direct integration.

First, a conformational isomeric state is assigned to each trough of low potential energy in the diad contour maps in Figures 2 and 3. Partial partition functions, z_k, average energies, $\langle E\rangle_k$, and average torsion angle values, $\langle \phi_j\rangle_k$, of the kth state are given by

$$z_k = \int_{\{\phi\}_k}\int_{\{\chi\}} \exp(-E/RT)\, d\phi\, d\chi \qquad (13)$$

$$\langle E\rangle_k = z_k^{-1}\int_{\{\phi\}_k}\int_{\{\chi\}} E\exp(-E/RT)\, d\phi\, d\chi \qquad (14)$$

$$\langle \phi_j\rangle_k = z_k^{-1}\int_{\{\phi\}_k}\int_{\{\chi\}} \phi_j \exp(-E/RT)\, d\phi\, d\chi, \quad j = i,\ i+1 \qquad (15)$$

where $\phi = [\phi_i,\phi_{i+1}]$, $\chi = [\chi_{i-1},\chi_{i+1},\chi'_{i-1},\chi'_{i+1},\ldots]$, and the integration range for main-chain torsion angles, $\{\phi\}_k$, is the area of the corresponding trough, while the range of the

Table IV
Results of Direct Integration for PS4MH Diads

	z			$\langle E \rangle$, kcal mol^{-1}			$\langle \phi_i \rangle$, $\langle \phi_{i+1} \rangle$, deg		
	300 K	400 K	500 K	300 K	400 K	500 K	300 K	400 K	500 K
meso									
|gt|	1.95	2.15	2.16	0.33	0.12	−0.08	113, 11	111, 13	110, 14
|tg|	1.82	1.80	1.75	−0.01	−0.08	−0.14	11, 112	14, 111	15, 110
|gg*|	0.10	0.21	0.32	1.86	1.71	1.57	114, 73	113, 73	113, 73
|g*g|	0.11	0.23	0.34	1.80	1.62	1.47	73, 113	72, 113	72, 112
|t*t|	0.06	0.13	0.18	1.80	1.53	1.31	53, 11	53, 11	53, 12
|tt*|	0.05	0.11	0.16	1.82	1.59	1.41	11, 53	12, 54	12, 54
|g*ḡ|	0.02	0.05	0.07	1.88	1.79	1.72	77, −110	77, −111	77, −111
|ḡg*|	0.02	0.04	0.07	2.14	2.02	1.92	−111, 76	−111, 76	−111, 76
|t*ḡ|	0.02	0.06	0.10	2.30	2.04	1.82	52, −120	51, −120	51, −120
|gt*|	0.03	0.06	0.11	2.35	2.09	1.84	−120, 52	−120, 52	−120, 51
racemo									
|tt|	1	1	1	0	0	0	10, 10	13, 13	15, 15
|gg|	1.50	2.06	2.35	0.83	0.63	0.42	110, 110	110, 110	110, 110
|t*g|, |gt*|	0.05	0.12	0.19	2.23	1.99	1.76	51, 115	51, 115	51, 115
|tg*|, |g*t|	0.04	0.11	0.18	2.21	2.00	1.79	12, 73	13, 72	14, 72
|ḡg*|, |g*ḡ|	0.02	0.06	0.10	2.52	2.29	2.07	−120, 75	−120, 75	−121, 75
|ḡt*|, |t*ḡ|	0.01	0.03	0.05	2.62	2.42	2.23	−110, 51	−110, 51	−110, 51

side-chain torsion angles, $\{\chi\}$, covers the entire range from 0° to 360° for each angle. The partial partition functions z_k can be used as elements of new statistical weight matrices $\mathbf{U''}_m$ and $\mathbf{U''}_r$, which contain now the contribution of mutual interactions of neighboring side groups. The differences in conformation space available to a side group in different conformations of the adjoining main-chain bonds are not properly taken into account in the elements of these $\mathbf{U''}$s, however, since the side groups (being located at the ends of the diads used for 13–15) enjoy too large a conformational freedom, independent of the diad conformation. The influence of the proximate main-chain conformations must be incorporated into the interdiad matrix $\mathbf{U'}$.

For the estimation of the elements of $\mathbf{U'}$ a triad is used. The main-chain torsion angles of the triad of the chosen stereostructure are assigned values of conformational isomeric states, obtained above with eq 15. The first and third side groups in the triad are assigned conformations found to give minimum energy in the diad computations above (in our applications these conformations always turned out to be such that the first and third side groups were "folded away" from the central, second side group). The entire triad is then kept rigidly in this conformation, except for the central side group; the central side group is rotated around all torsion angles in order to span all of its conformation space. The potential energy of the triad, averaged over all conformations of the central side group in a given main-chain conformation, is then obtained by

$$z' = \int_{\{\chi_{i-1}\}} \exp(-E/RT)\, d\chi_{i-1} \tag{16}$$

$$\langle E' \rangle = (z')^{-1} \int_{\{\chi_{i-1}\}} E \exp(-E/RT)\, d\chi_{i-1} \tag{17}$$

where $\chi_{i-1} = [\chi_{i-1}, \chi'_{i-1}, \ldots]$. From this average energy the averaged energies of the two diad conformations comprising the triad (calculated by eq 14) are subtracted, and the resulting "net energy" is used for the corresponding statistical weight in the matrix $\mathbf{U'}$.

A natural consequence of this procedure is the dependence of the interdiad matrix $\mathbf{U'}$ on diastereomerism in the main chain: we anticipate three distinct matrices, $\mathbf{U'}_{mm}$, $\mathbf{U'}_{mr}$, and $\mathbf{U'}_{rr}$ (and a fourth, $\mathbf{U'}_{rm} \neq \mathbf{U'}_{mr}$ for polymers with chiral side groups) that have to be evaluated.

The practical limitation of the method outlined above lies in the rapidly increasing number of conformations necessary for the evaluation of the integrals in eq 13–15 as the length of the side group, and with it the number of side-group torsion angles, increases. If integration is performed on an equidistant mesh, for instance, the number of conformations of which a calculation of the potential energy is necessary for the evaluation of $\mathbf{U''}_m$ is roughly $0.15(360°/\Delta\chi)^{2m+2}$, where m is the number of relevant torsion angles in a side group, $\Delta\chi$ is the spacing in the mesh, and the factor 0.15 designates the fraction of area of low energy in the maps in Figures 2 and 3. If $\Delta\chi$ is chosen as 10°, for instance, chains with two relevant side-group torsion angles (e.g., P1P, P4MP) require the inspection of more than 3×10^8 individual conformations. For PS4MH, with three side-group torsion angles, that number increases to more than 4×10^{11}; even the fastest of today's computers would be too slow by several orders of magnitude for such an undertaking. However, it is possible to reduce the number of conformations required significantly by using larger values for $\Delta\chi$, and by omitting a priori from consideration those ranges in χ which gives rise to excessively high energies and which therefore do not contribute significantly to the integrals in eq 13–15; in this fashion one can still obtain approximations for the statistical weight matrices for PS4MH, as we demonstrate here.

Application to Isotactic P4MP and Isotactic PS4MH. Application of the method of direct integration to P4MP and PS4MH required a series of exploratory calculations; grids of various mesh sizes and with different spacings were used in the integrations in eq 13–15, and the following argument values for torsion angles were chosen: ϕ_i, ϕ_{i+1}, grid of mesh size 10° in all areas of diad energy less than 6 kcal mol^{-1}; χ_{i-1}, χ_{i+1}, −140°, −120°, −100°, 100°, 120°, 140°; χ'_{i-1}, χ'_{i+1}, −140°, −120°, −100°, −20°, 0°, 20°; χ''_{i-1}, χ''_{i+1}, −120°, 0°, 120° (PS4MH only).

Even though this afforded only a very coarse sampling of conformation space, it still required the evaluation of more than 3×10^6 single diad conformations for both polymers considered. The trapezoidal rule was chosen for all integrations.

Results of the diad computations for PS4MH are shown in Table IV. The entries for the partial partition functions at temperatures of 300, 400, and 500 K are identified at these temperatures with the matrix elements in $\mathbf{U''}_m$ and $\mathbf{U''}_r$ (10 nonzero elements each, compare also eq 1). The values for the average torsion angles, listed in the three final columns of Table IV, lead to the adoption of rotational isomeric states at ϕ = 15° (t), 50° (t*), 75° (g*), 110° (g), and −115° (ḡ), in very close agreement with the values found for PP (see above and ref 41).

Table V
Intradiad Statistical Weight Matrices U'_{mm} for PS4MH, Obtained by Direct Integration[a]

At T = 300 K

0	0	0	0	0.210	0.051	0.562	0.003	0.003	0.207
0.001	0.010	0.102	0	0	0	0	0	0.191	0.035
0	0	0	0	0.010	0.002	0.001	0.001	0.028	0.002
0.017	0.058	0.001	0.001	0	0	0.271	0	0	0
0	0.006	0.001	0	0	0	0	0	0	0
0.002	0.002	0.024	0.014	1.0	0.298	0.077	0	0	0
0	0.001	0	0	0.146	0.047	0.024	0.015	0.119	0.011
0.005	0.046	0.035	0	0	0	0	0	0	0.389
0	0	0	0	0	0	0.031	0.001	0.001	0.041
0.001	0.010	0.006	0	0	0	0	0	0	0.120

At T = 400 K

0	0	0	0	0.255	0.085	0.553	0.011	0.009	0.253
0.004	0.051	0.186	0.002	0	0	0	0	0.375	0.109
0	0	0	0	0.027	0.007	0.006	0.005	0.040	0.007
0.025	0.124	0.004	0.003	0	0	0.355	0	0	0
0.003	0.030	0.003	0.002	0	0	0	0	0	0
0.006	0.010	0.046	0.031	1.0	0.401	0.151	0	0	0
0	0.005	0	0	0.252	0.103	0.067	0.051	0.177	0.031
0.018	0.146	0.070	0	0	0	0	0	0	0.573
0	0	0	0	0	0	0.061	0.004	0.003	0.073
0.004	0.037	0.015	0	0	0	0	0	0	0.207

At T = 500 K

0	0	0	0	0.290	0.115	0.542	0.026	0.018	0.281
0.012	0.127	0.272	0.006	0	0	0	0	0.537	0.208
0	0	0	0	0.050	0.015	0.014	0.013	0.049	0.016
0.035	0.191	0.009	0.008	0	0	0.419	0	0	0
0.008	0.077	0.009	0.008	0	0	0	0	0	0
0.013	0.026	0.068	0.050	1.0	0.471	0.220	0	0	0
0	0.016	0	0	0.346	0.160	0.119	0.102	0.218	0.057
0.039	0.272	0.108	0	0	0	0	0	0	0.717
0	0	0	0	0	0	0.088	0.010	0.006	0.098
0.010	0.082	0.026	0	0	0	0	0	0	0.285

[a] See text for details. Rows and columns are indexed in the order: |tt*|, |tg|, |t*t|, |t*ḡ|, |g*g|, |g*ḡ|, |gt|, |gg*|, |ḡt*|, |ḡg*|.

The elements of the isotactic interdiad statistical weight matrix, **U′**, were then estimated following the procedure described above. Integration over all degrees of freedom of the central side group in an otherwise rigid triad conformer (eq 16 and 17) were performed on regular meshes with uniform spacing of 20°. These calculations showed that the "net energy", obtained by subtracting the corresponding two average diad energies (from Table IV, for PS4MH) from the average triad energy, is strongly dependent not only on the conformation of the bonds immediately adjoining the central side group (i.e., bonds $i-1$ and i, see Figure 1) but also on the conformation of the bonds next to them (i.e., bonds $i-2$ and $i+1$, see Figure 1). Consequently, a *conformational isomeric state scheme* with diad conformations, leading to 10 × 10 statistical weight matrices, was adopted. The resulting matrix $\mathbf{U}'_{mm}$ for an isotactic triad of PS4MH, computed for temperatures of 300, 400, and 500 K, is displayed in Table V; states are indexed in the order |tt*|, |tg|, |t*t|, |t*ḡ|, |g*g|, |g*ḡ|, |gt|, |gg*|, |ḡt*|, |ḡg*|. The chirality of the side group makes conformations, which are usually of identical weight, unequal. The strongest discrepancy seems to appear between meso-|tg| and meso-|gt|, i.e., the "helical" diad conformations; still, the ratio between statistical weights is smaller than expected from the simple scheme (eq 6 and 11) (only 1.07 at 300 K, and 1.23 at 500 K). To make the intradiad matrices ($\mathbf{U}''_m$ and $\mathbf{U}''_r$) compatible with this scheme they are written as diagonal 10 × 10 matrices, the diagonal elements being taken from the correspondingly labeled entry in Table IV.

The interdiad matrices for triads of other than isotactic configuration ($\mathbf{U}''_{mr}$, $\mathbf{U}''_{rm}$, and $\mathbf{U}''_{rr}$ for PS4MH) were not calculated, since the experimental data available pertains almost exclusively to isotactic chains.

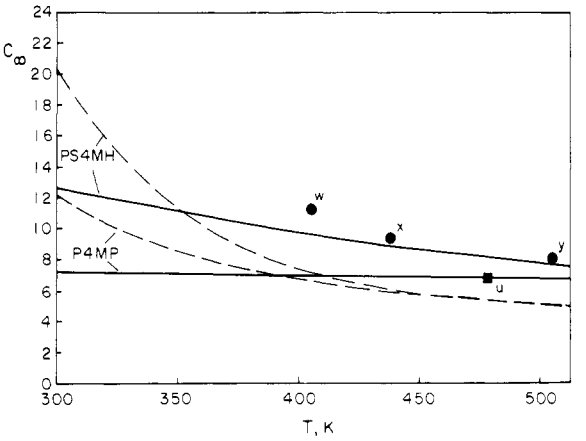

Figure 5. Characteristic ratios, $\lim_{n\to\infty} \langle r^2\rangle_0/nl^2$, for isotactic P4MP and PS4MH, calculated with the direct integration scheme: solid lines. Experimental points are taken from Figure 4. The dashed lines represent the calculations with the simple five-state scheme, taken from Figure 4.

Similar results have been obtained for P4MP. Here, the symmetry of the side group requires "symmetry" in the weights of rotational isomeric states; e.g., in $\mathbf{U}''_m$ the statistical weights for |tg| and |gt| must be identical, and this fact was used to monitor the accuracy of the computations. Results for P4MP are not displayed.

Characteristic Ratios. The characteristic ratios, C_∞, were calculated by using the standard generator matrix technique, with the 10 × 10 matrices obtained for isotactic P4MP and isotactic PS4MH, as described above and with the bond angles set to the values in Table I. Torsion angles

Table VI
Conformation Statistics for Isotactic PS4MH

	fraction of mono units[a]		
	300 K	400 K	500 K
in left-handed helical conformations (i.e., |gt|)	0.81	0.70	0.53
in right-handed helical conformations (i.e., |tg|)	0.03	0.11	0.24
in nonhelical conformations (all others)	0.16	0.19	0.23

	av sequence length[b]		
	300 K	400 K	500 K
left-handed helical conformations	6.5	5.3	3.9
right-handed helical conformations	1.5	2.0	2.8
nonhelical conformations	1.10	1.01	1.04

		probability of transition[c]		
from	to	300 K	400 K	500 K
left-handed	left-handed	0.84	0.62	0.42
	right-handed	0.16	0.38	0.58
right-handed	left-handed	0.99	0.98	0.91
	right-handed	0.01	0.02	0.09

[a] Fractions of monomeric units in different types of conformations. [b] Average sequence length of different types of conformations (in monomeric units). [c] Probabilities of transition from a helical conformation to another helical conformation; the number of intervening monomeric units in nonhelical conformations is not restricted.

were those derived from the averaging in eq 15, i.e., ϕ = 15° (t), 50° (t*), 75° (g*), 110° (g), and −115° ($\bar{g}$). The results are displayed in Figure 5. Heavy lines show the values for C_∞ obtained by direct integration, dots and squares are experimental values taken from Figure 4, and dashed lines are the computed results from the simple rotational isomeric state scheme, also displayed in Figure 4. Agreement between calculation and experiment is much improved by direct integration and seems to support the concepts imbedded in it. Especially noteworthy is the drastic reduction of the estimated temperature coefficient at lower temperatures in going from the simple rotational isomeric model to the results from direct integration.

Conformation Statistics for Isotactic PS4MH. In earlier investigations of isotactic vinyl polymers with chiral side groups,[27-32] and especially of PS4MH, attention was focused on the helical sections of chain conformations. Usually it was assumed that a left-handed helical section would have to be followed by a right-handed helical section, and vice versa, and that the population of nonhelical conformations was insignificant. The statistical weight matrices of order 10 × 10 obtained above ($\mathbf{U}'_{mm}$ and $\mathbf{U}''_{m}$) allow now the compilation of conformation statistics of any desired sequence, following standard procedures.[48] A priori probabilities for conformational sequences one and two bonds in length were computed, and conditional probabilities for the transition from one conformation to another were obtained from these values.[48] The fractions of diads in helical sections and in nonhelical sections, and the average sequence lengths of these conformations, are given in Table VI.

The left-handed helical conformation is by far the preferred diad conformation, comprising 81% of all diads at 300 K, and still 53% at 500 K. In contrast, the right-handed helical diad conformations are rather rare at 300 K; with increasing temperature, however, they increase rapidly in frequency of occurrence and surpass at 500 K the nonhelical conformation (i.e., the sum of all diads not in |tg| or |gt|) which do not gain much from an increase in temperature. The average sequence length of the helical segments corresponds roughly to the frequency of occurrence of diads in these conformations; but the nonhelical conformations seem to most often occur in isolated diads. These values indicate that, even though helical conformations comprise 77–84% of all diad conformations, a system in which left-handed and right-handed segments alternate is not in agreement with the values computed. We therefore calculated the probabilities of transition from a helical segment of given handedness to another helical segment (regardless of the length of the nonhelical section between them). These values are also listed in Table VI. It is astonishing to realize that at lower temperatures the end of a left-handed helical section will most probably lead again to a left-handed helix, while this tendency is strongly diminished, and even reversed, as temperature increases. From right-handed sections, however, one usually will go to a left-handed section.

Conclusions

Comparison between calculation and experiment for the characteristic ratio of isotactic poly(α-olefins), shown in Figure 4, led us to conclude that Abe's method of taking account of the influence of articulated side chains on the statistical weights of main-chain rotational isomeric states is accurate and useful for short side chains. Experimental results for PP and P1B are very well reproduced without the benefit of adjustable parameters. Chains with three consecutive carbon atoms in the side chain (P1P and P4MP) are marginal cases; calculations give acceptable results. For longer chains, i.e., PS4MH, this method fails, however. It is our contention that this failure is due to an increased frequency of overlaps between neighboring side chains, which is ignored in models disregarding third and higher order interactions. In reality the side chains mutually exclude each other from otherwise accessible space. Of course, the longer the side chain, the more relevant this space exclusion must become. We therefore predict that the simple rotational isomeric state scheme will generally fail for vinyl polymers with long side chains of comparable "flexibility".

The method of direct integration, introduced above for the numerical evaluation of the statistical weights of chains with longer side groups, accounts properly for the interdependences between adjacent side groups. Its application to P4MP and PS4MH gives excellent agreement between experiment and calculation (see Figure 5) and substantiates our contention of "mutual overlap". The method is limited by the amount of computational work required. The amount of numerical effort increases exponentially with the number of rotational degrees of freedom in the side group. Even for PS4MH the amount of work is so high that only relatively approximate computations were feasible (giving, however, quite satisfactory results). For vinyl polymers with flexible side chains that are substantially longer than those of PS4MH the evaluation of the conformational characteristics is therefore still an unsolved problem.

Acknowledgment. We thank Professor P. Pino of the Institut für Polymere at the ETH in Zürich for his interest in our work. Partial support comes from the Texaco-Mangelsdorf Associate Professorship at MIT.

References and Notes

(1) Bunn, C. W.; Holmes, D. R. *Discuss. Faraday Soc.* **1958**, *25*, 95.
(2) Natta, G.; Corradini, P.; Bassi, I. W. *Gazz. Chim. Ital.* **1959**, *89*, 784.
(3) Petraccone, V.; Pirozzi, B.; Frasci, A.; Corradini, P. *Eur. Polym. J.* **1976**, *12*, 323.
(4) Cojazzi, G.; Malta, V.; Celotti, G.; Zannetti, R. *Makromol. Chem.* **1976**, *177*, 915.

(5) Moser, M.; Boudeulle, M. *J. Polym. Sci., Polym. Phys. Ed.* **1978**, *16*, 971.
(6) Kusanagi, H.; Takase, M.; Chatani, Y.; Tadokoro, H. *J. Polym. Sci., Polym. Phys. Ed.* **1978**, *16*, 131.
(7) Corradini, P. "The Stereochemistry of Macromolecules"; Ketley, A. D., Ed.; Marcel Dekker: New York, 1968; Part III, p 1.
(8) Miller, R. L. In "Polymer Handbook", 2nd ed.; Brandrup, J., Immergut, E. H., Eds.; Wiley: New York, 1974.
(9) Tadokoro, H. "Structure of Crystalline Polymers"; Wiley: New York, 1979; Chapter 7.
(10) Natta, G.; Corradini, P.; Ganis, P. *J. Polym. Sci.* **1962**, *58*, 1191.
(11) DeSantis, P.; Giglio, E.; Liquori, A. M.; Ripamonti, A. *J. Polym. Sci., Part A* **1963**, *1*, 1383.
(12) Tadokoro, H.; Tai, K.; Yokoyama, M.; Kobayashi, M. *J. Polym. Sci., Polym. Phys. Ed.* **1973**, *11*, 825.
(13) Corradini, P.; Petraccone, V.; Pirozzi, B. *Eur. Polym. J.* **1976**, *12*, 831.
(14) Ajo, D.; Granozzi, G.; Zannetti, R. *Makromol. Chem.* **1977**, *178*, 2471.
(15) Kinsinger, J. B.; Hughes, R. E. *J. Phys. Chem.* **1959**, *63*, 2002.
(16) Krigbaum, W. R.; Kurz, J. E.; Smith, P. J. *J. Phys. Chem.* **1961**, *65*, 1984.
(17) Kinsinger, J. B.; Hughes, R. E. *J. Phys. Chem.* **1963**, *67*, 1922.
(18) Mark, J. E.; Flory, P. J. *J. Am. Chem. Soc.* **1965**, *87*, 1423.
(19) Nakajima, A.; Saijyo, A. *J. Polym. Sci., Part A-2* **1968**, *6*, 735.
(20) Heatley, F.; Salovey, R.; Bovey, F. A. *Macromolecules* **1969**, *2*, 619.
(21) Sastry, K. Satyanarayana; Patel, R. D. *Eur. Polym. J.* **1969**, *5*, 79.
(22) Moraglio, G.; Gianotti, G. *Chim. Ind. (Milan)* **1973**, *55*, 163 and references cited therein.
(23) Tani, S.; Hamada, F.; Nakajima, A. *Polym. J.* **1973**, *5*, 86.
(24) Neuenschwander, P.; Pino, P. *Eur. Polym. J.* **1983**, *19*, 1075.
(25) Hamada, F.; Flory, P. J., unpublished results (according to notes in ref 35 and 41).
(26) Inagaki, H.; Miyamoto, T.; Ohta, S. *J. Phys. Chem.* **1966**, *70*, 3420.
(27) Pino, P.; Ciardelli, F.; Lorenzi, G. P.; Montagnoli, G. *Makromol. Chem.* **1963**, *61*, 207.
(28) Pino, P. *Adv. Polym. Sci.* **1965**, *4*, 363.
(29) Pino, P.; Salvadori, P.; Chiellini, E.; Luisi, P. L. *Pure Appl. Chem.* **1968**, *16*, 469.
(30) Birshtein, T. M.; Luisi, P. L. *Vysokomol. Soedin.* **1964**, *6*, 1238.
(31) Allegra, G.; Corradini, P.; Ganis, P. *Makromol. Chem.* **1966**, *90*, 60.
(32) Birshtein, T. M.; Ptitsyn, O. B. "Conformation of Macromolecules"; Interscience: New York, 1966.
(33) Abe, A. *J. Am. Chem. Soc.* **1968**, *90*, 2205.
(34) Abe, A. *J. Am. Chem. Soc.* **1970**, *92*, 1136.
(35) Abe, A. *Polymer J.* **1970**, *1*, 232.
(36) Mattice, W. L. *Macromolecules* **1975**, *8*, 644.
(37) Mattice, W. L. *Macromolecules* **1977**, *10*, 1171.
(38) Abe, A.; Jernigan, R. L.; Flory, P. J. *J. Am. Chem. Soc.* **1966**, *88*, 631.
(39) Flory, P. J.; Mark, J. E.; Abe, A. *J. Am. Chem. Soc.* **1966**, *88*, 639.
(40) Flory, P. J. "Statistical Mechanics of Chain Molecules"; Interscience: New York, 1966; Chapter VI.
(41) Suter, U. W.; Flory, P. J. *Macromolecules* **1975**, *8*, 765.
(42) Suter, U. W. *J. Am. Chem. Soc.* **1979**, *101*, 6481.
(43) Suter, U. W.; Saiz, E.; Flory, P. J. *Macromolecules* **1983**, *16*, 1317.
(44) Flory, P. J.; Sundararajan, P. R.; DeBolt, L. C. *J. Am. Chem. Soc.* **1974**, *96*, 5015.
(45) It was assumed that the g* conformation is characterized by the same first-order statistical weight σ as the g conformation. The error thus introduced is small since g* occurs only in combination with strong second-order interactions and its first-order parameter is always multiplied with at least ω, the combined statistical weight being small.
(46) Flory, P. J. *Macromolecules* **1974**, *7*, 381.
(47) Moraglio, G.; Gianotti, G. *Eur. Polym. J.* **1969**, *5*, 781.
(48) Reference 40, pp 73-92.

Effect of Alkyl Group Size on the Cooperativity in Conformational Transitions of Hydrophobic Polyacids

Benjamin W. Barbieri and Ulrich P. Strauss*

Department of Chemistry, Rutgers, The State University of New Jersey, New Brunswick, New Jersey 08903. *Received July 3, 1984*

ABSTRACT: The effect of alkyl group size on the cooperativity of the conformational transition of hydrolyzed copolymers of maleic anhydride and alkyl vinyl ethers, observed by potentiometric titration, has been studied. An improved method for estimating the cooperative unit size yielded values of 19 and 13 for the butyl and pentyl copolymers, respectively, in 0.2 M LiCl. Two other, more qualitative, treatments of the data confirmed this inverse relationship between the cooperativity and the alkyl group size. The apparent contrast with the direct relationship between micelle and hydrocarbon size usually found for ordinary amphiphiles is attributed to differences in the ionization ranges in which the transitions of the copolymers occur.

Introduction

The hydrolyzed 1-1 copolymer of maleic anhydride and butyl vinyl ether undergoes a conformational transition upon ionization.[1] We have recently shown that this transition can be described in terms of a cooperative breakup of uniformly sized small micelles formed from adjacent chain elements and have developed a method for estimating the size of these micelles from potentiometric titration data for the case where the micelles are much smaller than the polymer.[2]

During the study to be reported in this paper we were surprised to find that the micelle size characterizing the conformational transition of the corresponding pentyl copolymer was smaller than that of the butyl copolymer. In the course of our investigation we developed an improved method for estimating micelle sizes. We shall begin with a brief description of this refined method.

Modified Method for Evaluating Cooperative Unit Size

For a large polymer chain in which noninteracting micelles (each containing n adjacent repeat units) and random coil portions of any size alternate, the negative standard molar free energy of forming a micelle from n adjacent residues obeys the equation[2]

$$\frac{\Delta G^\circ_{mic}}{RT} = \ln \frac{1-\theta}{n\theta + (1-\theta)} - n \ln \frac{n\theta}{n\theta + (1-\theta)} \quad (1)$$

The quantity θ is the fraction of residues in the random coil form, obtained from the relation[1,3]

$$\theta = (\alpha - \alpha_m)/(\alpha_r - \alpha_m) \quad (2)$$

where α, α_m, and α_r are the degrees of deprotonation of the actual polyacid and its hypothetical micellar and random

0024-9297/85/2218-0411$01.50/0